

Toward the predictability of meteotsunamis in the Balearic Sea using regional nested atmosphere and ocean models

Lionel Renault,¹ Guillermo Vizoso,² Agustin Jansá,³ John Wilkin,⁴ and Joaquin Tintoré^{1,2}

Received 4 March 2011; revised 29 March 2011; accepted 30 March 2011; published 18 May 2011.

[1] Meteotsunamis are oceanic waves that possess tsunami-like characteristics but are meteorological in origin. In the western Mediterranean, travelling atmospheric pressure oscillations generate these long oceanic surface waves that can become amplified and produce strong seiche oscillations inside harbors. We analyze a June 2006 meteotsunami event in Ciutadella harbor (Menorca Island, Spain), studying numerically the phenomenon during its full life cycle, from the early atmospheric stages to the atmosphere-ocean resonant phase and the final highly amplified harbor oscillation. The Weather Research Forecast (WRF) atmospheric model adequately reproduces the development of a convective nucleus and also reproduces the induced atmospheric pressure oscillations moving at a speed of 27 m/s. The oceanic response is studied using the Regional Ocean Modeling System (ROMS), forced by the WRF pressure field. It shows an inverse barometer wave front in the open ocean progressively amplified through resonant interactions in the different shelf and coastal regions. The predictive capability of this new WRF/ROMS modeling approach is then discussed. **Citation:** Renault, L., G. Vizoso, A. Jansá, J. Wilkin, and J. Tintoré (2011), Toward the predictability of meteotsunamis in the Balearic Sea using regional nested atmosphere and ocean models, *Geophys. Res. Lett.*, 38, L10601, doi:10.1029/2011GL047361.

1. Introduction

[2] Meteotsunamis are long-period oceanic waves that possess tsunami-like characteristics but are meteorological in origin. They occur in oceans all over the world, usually under their local names such as “Rissaga” [*Ramis and Jansá, 1983; Tintoré et al., 1988; Gomis et al., 1993*] in Ciutadella harbor (Menorca Island, Spain). The sea level oscillation during a Rissaga event corresponds to the oceanic response to some atmospheric gravity waves [*Ramis and Jansá, 1983; Monserrat et al., 1991a*] and/or to convective pressure jumps [*Jansá, 1986; Monserrat et al., 2006*].

[3] The amplification mechanism is now well established [*Monserrat et al., 1991b; Liu et al., 2003; Vilibić et al., 2008*]: in essence, when the speed of propagation of the atmospheric disturbance (U) equals the oceanic local gravity wave speed (c), the Froude number (U/c) equals 1 (Figure 1b)

and a Proudman resonance [*Proudman, 1929*] amplifies the open ocean inverse barometer response. The amplified oceanic gravity wave is then followed by a harbor seiche resonance at Ciutadella and generates a Rissaga, with typical final amplitude of the order of 0.5 to 1 meter and period of around 10 minutes. Rissaga events typically occur several times a year (mainly in summer) and do not generally cause major damage in the harbor, however, destructive Rissaga events do occasionally occur. In such cases, the amplitude is 2 or even up to 5 meters. Inside the harbor, such strong events cause devastating damage to boats and harbor facilities. The last major Rissaga event at Ciutadella, the most important in 20 years, occurred on 15 June 2006, with oscillations of about four meters, as reported by eyewitnesses. It caused a catastrophic drying of a significant part of the harbor with more than 35 boats sunk and about 100 severely damaged [*Jansá et al., 2007; Monserrat et al., 2006*]. The total economic cost was estimated to reach tens of millions of Euros. Unfortunately, only two microbarographs at Palma de Mallorca and Menorca Airports were available to monitor the atmospheric pressure oscillations that gave rise to this event. The main oceanic features of the Rissaga have been studied numerically by *Vilibić et al. [2008]* using as forcing a synthetic atmospheric disturbance coincident with observations. Atmospheric features of meteotsunamis have also been assessed numerically in a few studies [e.g., *Belušić et al., 2007; Šepić et al., 2009; Tanaka, 2010*]. However, no previous study of meteotsunamis has addressed the numerical simulation of the phenomenon during all its life cycle, from the initial synoptic conditions and the induced atmospheric pressure disturbances to the final harbor amplified oscillation.

[4] Currently, forecasting Rissaga events is carried out on a routine basis by the Spanish State Meteorological Agency (AEMET) using a qualitative alert system based on the analysis of the synoptic atmospheric conditions [*Jansá, 1990*]. However, such a system cannot quantitatively predict the Rissaga intensity and some of the alerts are not associated with strong harbor oscillations. Therefore, further investigation on the origin, amplification and predictive capability is needed to meet this scientific challenge.

[5] In this study, for the first time, nested atmospheric and oceanic models were implemented over the Balearic Sea and evaluated in the context of the 2006 extreme Rissaga event. The main objectives were to demonstrate the capability of numerical models to reproduce the atmospheric and oceanic processes involved during meteotsunami generation and amplification, and also to discuss the development of steps towards improvement of the predictive capability for the Menorca Rissaga and other meteotsunami events, using similar modeling systems.

[6] The paper is organized as follows: Section 2 provides a description of the atmospheric and oceanic models used.

¹SOCIB, ICTS, Palma de Mallorca, Spain.

²IMEDEA (UIB, CSIC), Esporles, Spain.

³AEMET, Palma de Mallorca, Spain.

⁴Institute of Marine and Coastal Sciences, Rutgers, State University of New Jersey, New Brunswick, New Jersey, USA.

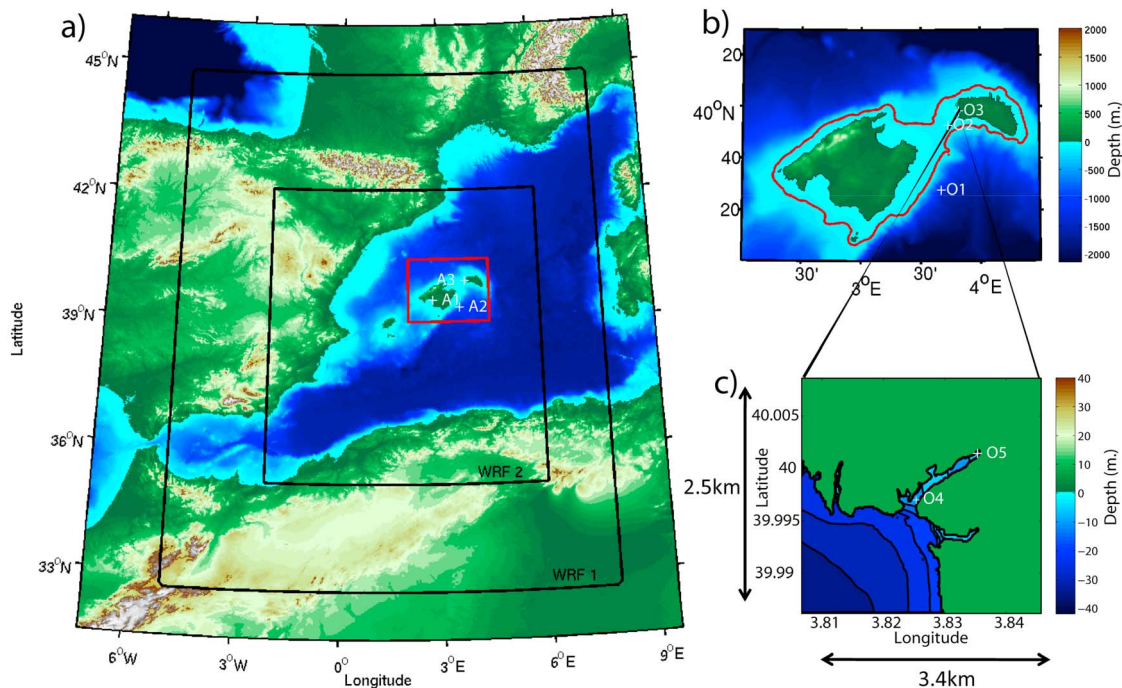


Figure 1. Model domains and topography. (a) Black boxes indicate the coarse (WRF1) and fine (WRF2) atmospheric model domains; the red box indicates the first parent ROMS ocean model domain. A1, A2 and A3 represent the atmosphere control points studied in Figures 2 and 3. (b) The first parent ROMS domain. O1, O2 and O3 represent the control points studied in Figure 4. The color represents the topography and ocean bathymetry and the red contour highlights the region where the Froude number is around 1 for an atmospheric wave velocity of 27 ms^{-1} . (c) The embedded ROMS domain. O4 and O5 are the control points studied in Figures 3 and 4, the black arrows indicate the child domain dimensions in km.

Section 3 describes the observations from the June 2006 event and Section 4 presents the main results from the atmospheric model and the oceanic response. The results are then discussed in Section 5, where the conditions under which the predictive capability of these models adds to and could improve the current forecasting system are also addressed.

2. The Models

2.1. Atmospheric Model

[7] The Weather Research and Forecasting (WRF) model (v3.2) [Skamarock *et al.*, 2008] has been implemented in a 2 nested grid configuration. The largest domain approximately covers the western Mediterranean basin with a horizontal resolution of 20 km while the inner domain covers the area that corresponds to the eastern part from Africa to the Balearic Islands, with a horizontal resolution of 4 km (see Figure 1a). The coarser grid reproduces the large-scale synoptic features that force the local dynamics in the second grid at each time step. The simulations are performed using a two-way nesting technique, starting at 0000 UTC, 13 June 2006 and lasting 72 h. Ninety-seven vertical levels are employed, more closely distributed in the lower levels to adequately resolve the characteristic inversion layer associated with Rissaga phenomena [Ramis and Jansá, 1983; Jansá, 1986]. Initial state and boundary conditions every six hours are prescribed from the synoptic atmospheric conditions as obtained from the NCEP FNL analysis (<http://dss.ucar.edu/datasets/ds083.2>). The following parameterization schemes were found to provide better agreement with observations and were therefore used:

the WRF SM5-class microphysics scheme [Skamarock *et al.*, 2008]; the Kain cumulus parameterization [Skamarock *et al.*, 2008] on the coarser grid (implicit on the inner grid); the MYNN2 scheme [Skamarock *et al.*, 2008] Planetary Boundary Layer (PBL). The WRF model has been implemented in previous studies to simulate the atmospheric features of various meteotsunamis [e.g., Šepić *et al.*, 2009; Tanaka, 2010].

2.2. ROMS Ocean Model

[8] The oceanic simulations were performed with the Rutgers version of the Regional Ocean Modeling System (ROMS, www.myroms.org). ROMS is a 3D free-surface, split-explicit primitive equation model with Boussinesq and hydrostatic approximation. The reader is referred to the work of Shchepetkin and McWilliams [2005] for a description of the numerical algorithms. Two embedded domains were implemented (refer to Figures 1b and 1c). The parent domain covers the Balearic Islands with a horizontal resolution of 1 km (256×200 grid points). Bottom topography is derived from the Smith and Sandwell product [Smith and Sandwell, 1997]. The higher resolution nested domain covers the Western part of Menorca with a resolution of 10m (401×302 grid points), allowing a good sampling of the Ciutadella harbor coastline. The bathymetry was derived from a high-resolution bathymetry provided by the University of Cantabria. The model has 20 vertical levels in terrain following coordinates. The boundary and initial conditions of the parent domain are prescribed analytically, and include vertically homogeneous temperature and salinity such that the configuration is almost 2-dimensional; the

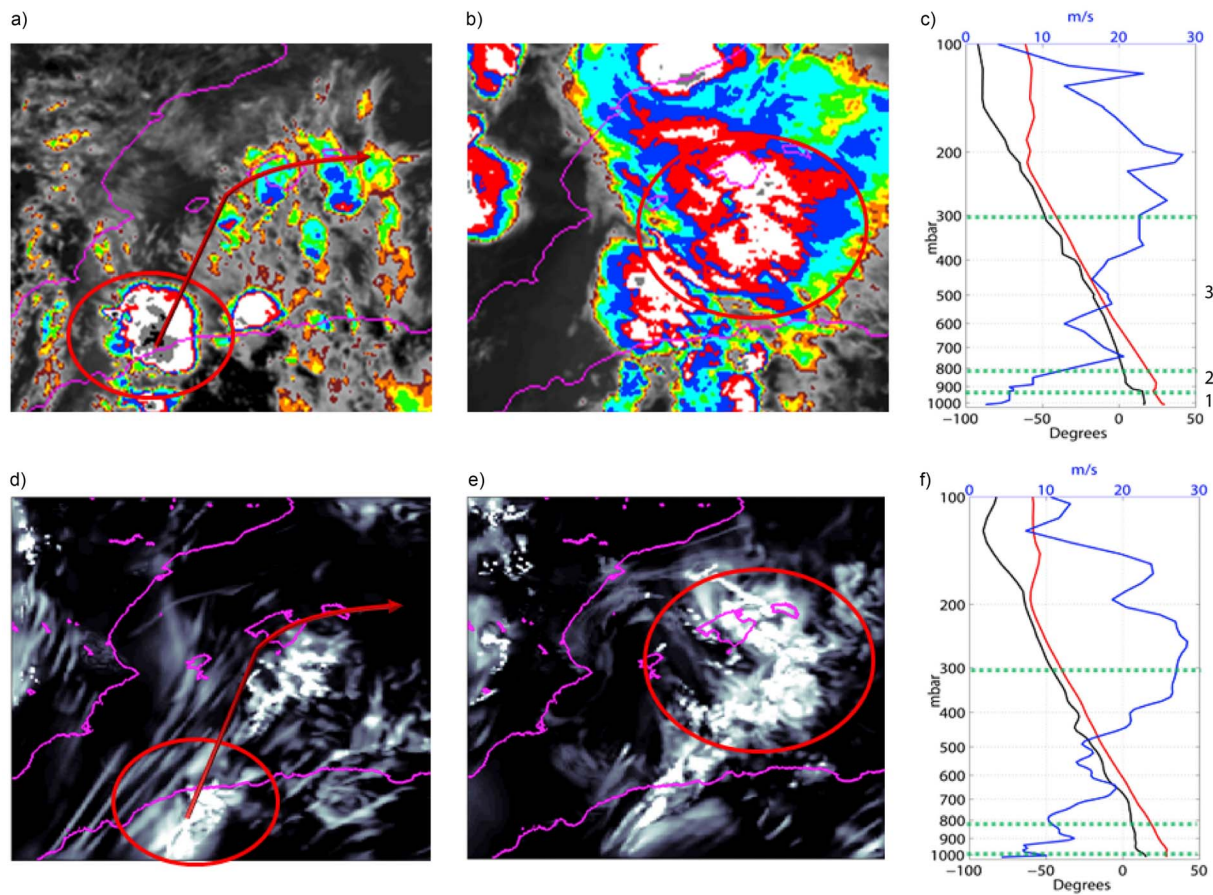


Figure 2. (a) Satellite infrared image 1400UTC 15 June 2006. (b) Satellite infrared image 1900UTC 15 June 2006. (c) Vertical profile from the Palma de Mallorca radiosounding 1200UTC 15 June 2006. The red (black) lines show temperature (dew point) in degrees Celsius and the blue line the wind speed (m/s). The dotted green lines and the black numbers highlight the three layer structure described in the section 3. (d) Simulated vertically integrated water content 1500UTC 15 June 2006. (e) The same as Figure 2d at 2000UTC. (f) The same as Figure 2c but from the model. In Figures 2a, 2b, 2d, and 2e the red circles highlight the convective system and the red arrows the convective system trajectory.

absence of density stratification eliminates baroclinic pressure gradients but the velocity can still be vertically sheared consistent with the quadratic drag parameterization of bottom drag. The embedded domain boundary conditions are derived from the parent model using integrated current and sea surface elevation. The model is forced every 2 minutes by the WRF Sea Level Pressure (SLP). A more complex configuration using WRF surface wind forcing in addition to SLP was also run to test the wind impact on the ocean response.

3. The 15 June 2006 Event: Description From Observations

[9] The synoptic atmospheric situation over the western Mediterranean Sea on 15 June 2006 can be described as a three-layer structure [Jansá *et al.*, 2007]. It is well apparent in Figure 2c, which presents the vertical profiles (obtained by the Palma de Mallorca radiosounding) for air temperature, air temperature dew point and wind speed just before the Rissaga (15 June, 1200UTC). The first layer (1) is characterized by low level Mediterranean air, close to the surface. The second layer (2), around 850 hPa, is separated from (1) by an inversion layer and is characterized by the

presence of warm African air. Above this layer, there is colder air, with strong thermal gradient between the core of the warmest air (850 hPa) and the core of the coldest air (500 hPa); the depth of this third layer (3) is approximately between 750–800 hPa and 300–500 hPa (levels marked by the presence of strong south-westerly winds). As a result, this third layer is weakly stable and is marked by a vertical wind shear across it (see Figure 2c), favoring therefore gravity waves formation and even convection [Jansá *et al.*, 2007].

[10] Figures 2a and 2b show the infrared satellite images at 1400UTC and 1900UTC. In essence, on 15 June 2006, at 1400UTC, a deep convective nucleus developed near the African coast (1°E – 36°N) and travelled from SW to NE (see red circle and arrow on Figures 2a and 2b) with a velocity of 26 m/s (estimated from the satellite images by Belušić and Mahović's [2009] method). It was associated with weak precipitation and a squall line with wind gusts reaching up to 20–25 m/s, lasting only several minutes [Jansá *et al.*, 2007]. Around 1900UTC, the convective nucleus traveled across the Balearic Islands. As indicated by the pressure measurements at the Palma de Mallorca and Menorca airports (AEMET, Figure 3c), a sudden pressure jump of 5 hPa

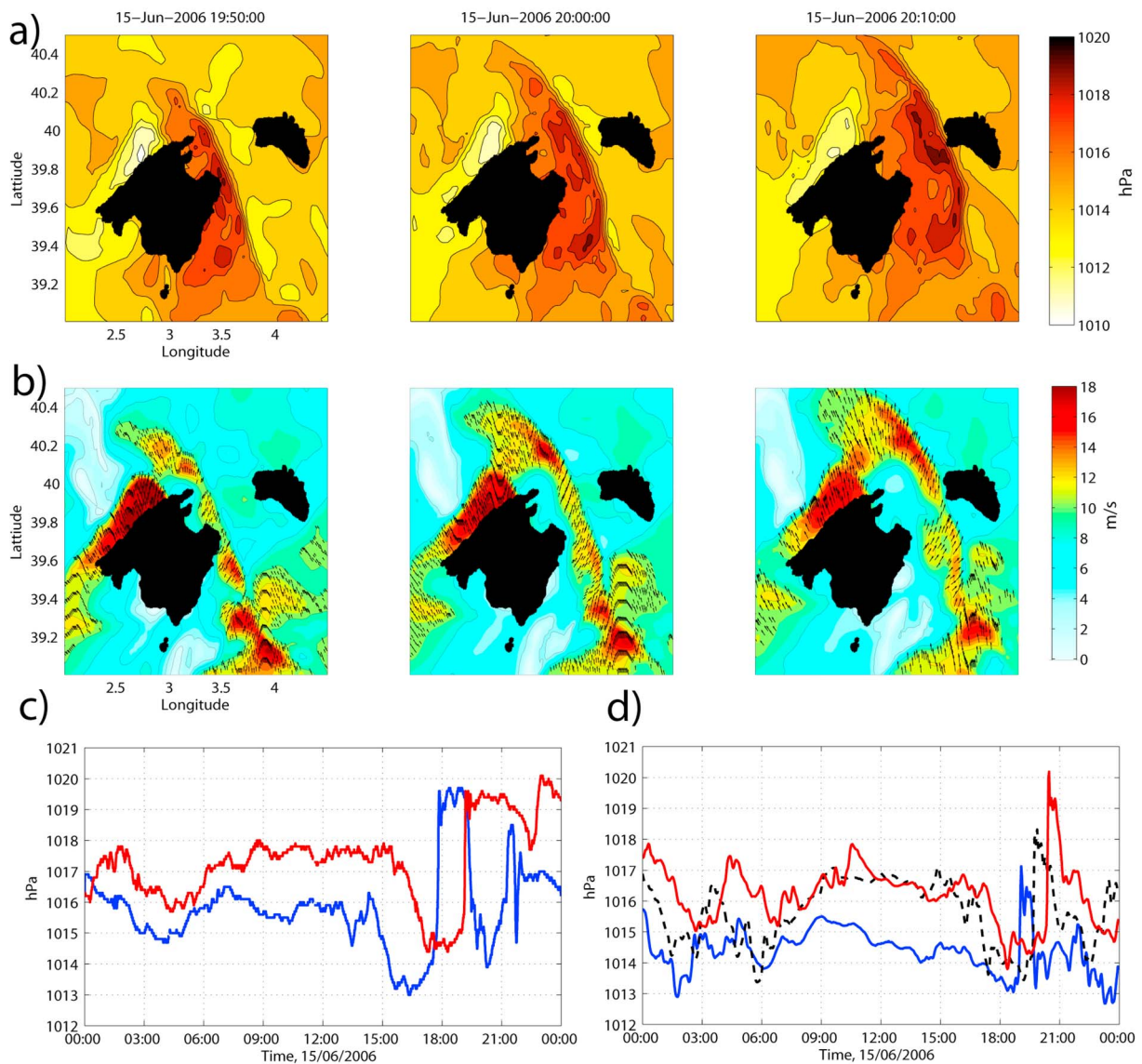


Figure 3. (a) SLP snapshots each 10 minutes from 1950 UTC 15 June 2006. (b) The same as Figure 3a for the surface wind speed and direction. The color fields represent the wind speed and the arrows the wind direction (only wind >12 m/s). (c) Temporal evolution of the measured sea level pressure at the points A1 and A3 (lines blue and red) represented in Figure 1. (d) Temporal evolution of the simulated sea level pressure at the points A1, A2 and A3 (lines blue, black and red) represented in Figure 1.

accompanied the squall line. This pressure jump travelled across the channel between Mallorca and Menorca at a velocity of 25 m/s [Vilibić *et al.*, 2008] which, as indicated by Belušić and Mahović [2009] does not necessarily match the cloud top velocity. Across the channel, the travelling pressure generated an oceanic longwave through Proudman resonance that in turn induced the seiche into the Ciutadella harbor, a process well described by Vilibić *et al.* [2008].

4. Model Results

[11] The atmospheric simulation reproduced the main atmospheric features just described for the 15 June 2006 event with a delay of one hour. Figures 2d and 2e represent the integrated atmospheric water content at 1500UTC and

2000UTC. In good agreement with the Figures 2a and 2b, the development of a clear convective nucleus near the African coast (1°E–36°N) is simulated by the model and travelled until the Balearic Islands (see red arrow on Figure 2d) with a velocity of 27 m/s (estimated by Belušić and Mahović [2009] method on the simulated cloud fields). Figure 3a represents three snapshots of the simulated SLP over the Balearic Islands (around 2000UTC) and Figure 3c represents the SLP time-series at the three locations indicated on Figure 1: near Palma (A1), at the channel entrance (A2), and near Maó (Menorca) (A3). Associated with the simulated convective nucleus, a sudden pressure jump of 5 hPa travels across the channel with a velocity of 27 m/s (using Gautama and Van Hulle [2002] optical flux method). Although the simulated disturbance is a little bit faster than the observed one and with

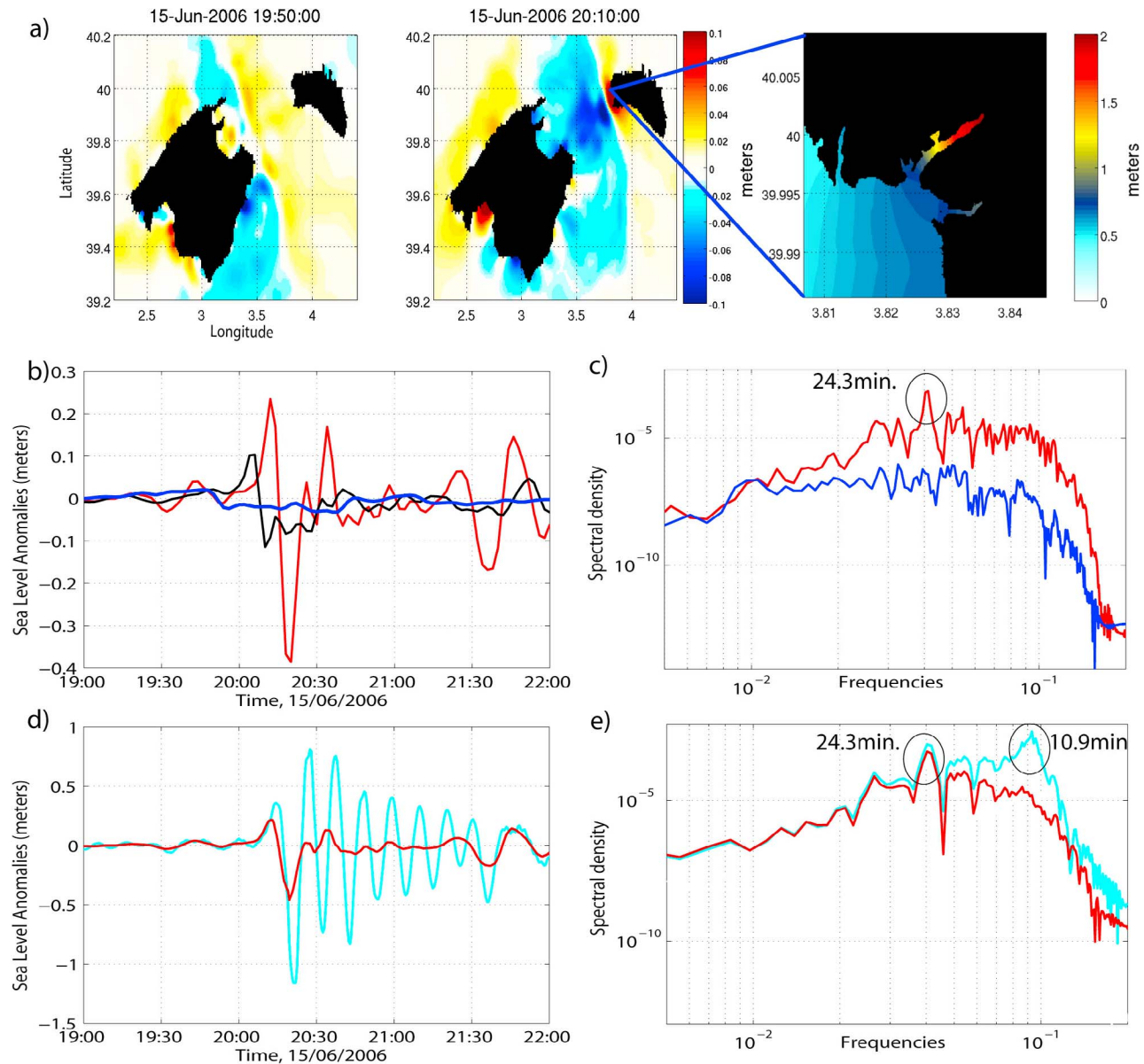


Figure 4. Oceanic response to the June 2006 Rissaga. (a) SLA snapshots at the same time as in Figure 3a and maximum difference of SLA during the Rissaga event in the Ciutadella Harbor. (b) The blue, black and red lines represent respectively the SLA at the points O1, O2 and O3. (c) The red (blue) line represents the spectrum of the SLA timeseries at the point O3 (O1). (d) The same as Figure 4b but for the points O4 (red line) and O5 (cyan line). (e) The same as Figure 4c but for the points O4 (red line) and O5 (cyan line).

a slight lesser rate, these results are in good agreement with the observations (refer to Figure 3c).

[12] Figure 3b shows the simulated sea surface wind associated with the SLP snapshots presented in Figure 3a. One can note the presence of a squall line with wind reaching up to 15 m/s at the surface and 25 m/s at the top of the inversion layer (not shown). To compare the atmospheric simulated vertical structure to the observations (Figure 2c), Figure 2f presents the simulated dew point, air temperature and wind speed just before the Rissaga near Palma de Mallorca (15 June 1200UTC). Although the simulated inversion layer is too low compared to observations (refer to Figure 2c), the presence of the African dry air (layer 2 on Figures 2c and 2f) and the unstable layer (layer 3

on Figures 2c and 2f) above it characterized by a strong wind shear is reasonably simulated. Moreover, the presence of strong winds at the upper levels (up to 25 m/s) is well simulated by the model (refer to Figures 2c and 2f).

[13] The oceanic response to the simulated moving pressure jump consists of an isostatic inverse barometer effect generating barotropic shallow water gravity waves, which are intensified through different amplification and resonant processes. To illustrate this, Figure 4a presents three snapshots of the Sea Level Anomaly (SLA) showing the amplification of the adjusted sea level along the channel (Proudman resonance) and the associated harbor resonance (the natural seiche) of the Ciutadella Inlet and Figure 4b shows the SLA timeseries at points O1, O2 and O3 (see

Figure 1b). In deep water the ocean response is almost isostatic (5 cm). In the channel the response is amplified up to 10 cm due the Proudman resonance and at the mouth of the inlet, due to the combined Proudman resonance and topographical amplification, the maximum set-up and set-down reach about 25 cm and 40 cm. Inside the inlet, due to the harbor resonance, the trough-to-crest wave reaches up to 2 meters (Figures 4a and 4d) which is comparable to the simulations by *Vilibić et al.* [2008] but weaker than the wave amplitude described by the witnesses (4–5 meters).

[14] To compare the spectral properties of the simulated oceanic response with the literature, Figures 4c and 4d present the spectrum of the band-pass filtered (cutoff period $f_c = 60$ minutes and $f_c = 4$ minutes) SLA at points O1, O3, O4 and O5 (refer to Figures 1b and 1c). In good agreement with observational studies [*Garcies et al.*, 1996; *Marcos et al.*, 2004, 2009], the main interesting results are: (1) Over the channel, the spectral power of the SLA time-series increases due to the Proudman resonance. (2) The dominant period of the SLA at O3 and O5 (i.e., channel and entrance of the harbor) is around 24.3 minutes (compared to 24.4 minutes in the observations), which represents the shelf eigenfrequencies. (3) Inside the harbor, the main period is around 10.9 minutes (10.5 minutes in the observations), this being the main harbor eigenfrequency [*Rabinovich and Monserrat*, 1996; *Rabinovich et al.*, 1999; *Vidal et al.*, 2000; *Liu et al.*, 2003]. Inside the harbor, the oceanic longwave has frequencies matching the eigenfrequencies of the inlet, which induce the simulated large resonant seiche response. Finally, in good agreement with the observations and with *Vilibić et al.* [2008], the strongest currents, which caused the majority of the damage, are simulated in the middle of Ciutadella Inlet and reach up 180 cm/s (not shown).

5. Discussion, Predictive Capability and Concluding Remarks

[15] In this study, for the first time, we have implemented both atmospheric and oceanic models to assess the 15 June 2006 Rissaga extreme event. The model adequately reproduces the convective system and the pressure jump with an intensity comparable to that observed, but with a temporal lag of one hour. The oceanic model, forced by the simulated SLP, also realistically reproduces the main resonances that drive the oceanic response and the seiche into the Ciutadella harbor.

[16] We have found that, in agreement with observations, the convective nucleus was associated with strong wind gusts reaching up to 15 m/s at the sea surface. *Rabinovich* [2008], suggested that these wind gusts could play a secondary role to explain the Rissaga formation. In order to test this hypothesis, we used the same ROMS configuration and forced it by the WRF sea surface wind in addition to the SLP. The results are quite similar to those without wind forcing. Maximal oscillation into the harbor reaches 2 meters and maximum current is situated also in the middle of the Ciutadella inlet and reaches up 180 cm/s. Therefore, following our simulations, the wind does not seem to have a significant role in explaining the Rissaga.

[17] Differences between observations and simulations can be due to several factors. The atmospheric simulations exhibit a strong sensitivity to the initial and boundary conditions. Uncertainties due to their low temporal and spatial

resolution can also lead to some biases both in location and timing of the convective system or the gravity waves. A modeled disturbance located 30 km to the east of the actual feature, or with an inaccurate orientation would not give rise to strong oscillations in Ciutadella, while in reality there could be a significant event. In our case, the atmospheric model was initialized 48 hours before the Rissaga event by FNL analysis, and the WRF boundary conditions were updated every 6 hours. In other preliminary work, we repeated the simulation using the NCEP2 reanalysis product. The model simulated a convective system but it did not travel across the Balearic Islands. Improving the realism and spatial/temporal resolution of the initial and boundary conditions could therefore overcome some differences between model and observations. The atmospheric simulation results are also sensitive to the boundary layer (PBL) scheme chosen. Other Rissaga cases were simulated reasonably using the configuration presented in this study with other PBL schemes, but results suggest that PBL processes play a crucial role in determining the intensity of the SLP oscillations. They can vary from 20% to 40% in this extreme case. These differences would lead to different oceanic response in terms of oscillation amplitude in the harbor. Finally, some of the model/observation discrepancies could be due to the insufficient accuracy and spatial resolution of the bathymetry and coastline of the ROMS configuration. These uncertainties are a limitation on the modeling system and as a potential forecasting system and are the subject of on-going research. Nevertheless, the current Rissaga alert system [*Jansá*, 1990], is based on the analyses of synoptic conditions and does not allow quantitative prediction of the intensity of a meteotsunami, and sometimes gives erroneous alerts. A two-day forecasting system based on the configuration described in this study could improve the current alert system.

[18] Overall, the approach we considered here shows that under certain atmospheric conditions meteotsunamis associated with travelling atmospheric waves and/or convective systems can be forecasted. It is important to note that the use of standard meteorological forecast output at 3-hour intervals would not generate the meteotsunami in the ocean model. The pressure oscillation must be resolved to about 2 minutes in order to capture the sudden pressure change of order 0.3 hPa/min that appears to be required for sizeable Proudman resonance. Therefore, a dedicated high-resolution meteorological forecast is a prerequisite to successfully predict meteotsunamis. The realism of the simulation results here is encouraging and argues in favor of developing a high-resolution atmosphere-ocean forecasting system in this region.

[19] **Acknowledgments.** This work has been partially funded by COOL (CTM2006-12072/MAR), ECOOP (CTM2007-31006E) and SOCIB Modeling Facility whose support is gratefully acknowledged. The FNL data (<http://dss.ucar.edu/ds083>) are from the Research Data Archive (RDA) maintained by the Computational and Information Systems Laboratory (CISL) at the National Center for Atmospheric Research (NCAR). NCAR is sponsored by the National Science Foundation (NSF). The two anonymous reviewers are gratefully acknowledged for their helpful and constructive comments, which improved the quality of this study. The authors thank AEMET and the University of Cantabria/SENER (Spain) for providing, respectively, the atmospheric pressure record, radiosounding and satellite observations during the Rissaga event and bathymetry.

[20] The Editor thanks two anonymous reviewers for their assistance in evaluating this paper.

References

- Belušić, D., and N. S. Mahović (2009), Detecting and following atmospheric disturbances with a potential to generate meteotsunamis in the Adriatic, *Phys. Chem. Earth*, *34*(17–18), 918–927.
- Belušić, D., B. Grisogono, and Z. B. Klaić (2007), Atmospheric origin of the devastating coupled air–sea event in the east Adriatic, *J. Geophys. Res.*, *112*, D17111, doi:10.1029/2006JD008204.
- Garcies, M., D. Gomis, and S. Monserrat (1996), Pressure forced seiches of large amplitude in inlets of the Balearic Islands: 2. Observational study, *J. Geophys. Res.*, *101*(C3), 6453–6467, doi:10.1029/95JC03626.
- Gautama, T., and M. M. Van Hulle (2002), A phase-based approach to the estimation of the optical flow field using spatial filtering, *IEEE Trans. Neural Networks*, *13*(5), 1127–1136, doi:10.1109/TNN.2002.1031944.
- Gomis, D., S. Monserrat, and J. Tintoré (1993), Pressure forced seiches of large amplitude in inlets of the Balearic Islands, *J. Geophys. Res.*, *98*(C8), 14,437–14,445, doi:10.1029/93JC00623.
- Jansá, A. (1986), Marine response to mesoscale-meteorological disturbances: the June 21, 1984, event in Ciutadella (Menorca), *Rev. Meteorol.*, *7*, 5–29.
- Jansá, A. (1990), Servei experimental de predicció de rissagues, in *Les Rissagues de Ciutadella i Altres Oscil·lacions de Nivell de la Mar de Gran Amplitud a la Mediterrània*, pp. 85–91, Inst. Menorquí d'Estudis, Menorca, Spain.
- Jansá, A., S. Monserrat, and D. Gomis (2007), The Rissaga of 15 June 2006 in Ciutadella (Menorca), a meteorological tsunami, *Adv. Geosci.*, *12*, 1–4, doi:10.5194/adgeo-12-1-2007.
- Liu, P. L.-F., S. Monserrat, M. Marcos, and A. B. Rabinovich (2003), Coupling between two inlets: Observation and modeling, *J. Geophys. Res.*, *108*(C3), 3069, doi:10.1029/2002JC001478.
- Marcos, M., P. L.-F. Liu, and S. Monserrat (2004), Nonlinear resonant coupling between two adjacent bays, *J. Geophys. Res.*, *109*, C05008, doi:10.1029/2003JC002039.
- Marcos, M., S. Monserrat, R. Medina, A. Orfila, and M. Olabarrieta (2009), External forcing of meteorological tsunamis at the coast of the Balearic Islands, *Phys. Chem. Earth*, *34*(17–18), 938–947.
- Monserrat, S., A. Ibberson, and A. J. Thorpe (1991a), Atmospheric gravity waves and the “Rissaga” phenomenon, *Q. J. R. Meteorol. Soc.*, *117*, 553–570.
- Monserrat, S., C. Ramis, and A. J. Thorpe (1991b), Large-amplitude pressure oscillations in the western Mediterranean, *Geophys. Res. Lett.*, *18*, 183–186, doi:10.1029/91GL00234.
- Monserrat, S., A. B. Rabinovich, and B. Casas (1998), On the reconstruction of the transfer function for atmospherically generated seiches, *Geophys. Res. Lett.*, *25*(12), 2197–2200, doi:10.1029/98GL01506.
- Monserrat, S., I. Vilibić, and A. B. Rabinovich (2006), Meteotsunamis: Atmospherically induced destructive ocean waves in the tsunami frequency band, *Nat. Hazards Earth Syst. Sci.*, *6*, 1035–1051, doi:10.5194/nhess-6-1035-2006.
- Proudman, J. (1929), The effects on the sea of changes in atmospheric pressure, *Geophys. J. Int.*, *2*(4), 197–209, doi:10.1111/j.1365-246X.1929.tb05408.x.
- Rabinovich, A. B. (2008), *Seiches and Harbour Oscillations. Handbook of Coastal and Ocean Engineering*, edited by Y. C. Kim, World Sci., Singapore.
- Rabinovich, A. B., S. Monserrat, and I. V. Fine (1999), Numerical modeling of extreme seiche oscillations (“Rissaga waves”) in the vicinity of the Balearic Islands, *Oceanology, Engl. Transl.*, *39*, 12–19.
- Ramis, C., and A. Jansá (1983), Condiciones meteorológicas simultáneas a la aparición de oscilaciones del nivel del mar de amplitud extraordinaria en el Mediterraneo occidental [in Spanish], *Rev. Geofis.*, *39*, 35–42.
- Šepić, J., I. Vilibić, and D. Belušić (2009), Source of the 2007 Ist meteotsunami (Adriatic Sea), *J. Geophys. Res.*, *114*, C03016, doi:10.1029/2008JC005092.
- Shchepetkin, A. F., and J. C. McWilliams (2005), The regional oceanic modelling system (ROMS): A split-explicit, free-surface, topography-following-coordinate ocean model, *Ocean Modell.*, *9*, 347–404, doi:10.1016/j.ocemod.2004.08.002.
- Skamarock, W. C., J. B. Klemp, J. Dudhia, D. O. Gill, D. M. Barker, M. Duda, X. Y. Huang, W. Wang, and J. G. Powers (2008), A description of the advanced research WRF version 3, *NCAR Tech. Note NCAR/TN-475+STR*, Nat. Cent. for Atmos. Res., Boulder, Colo.
- Smith, W. H. F., and D. T. Sandwell (1997), Global seafloor topography from satellite altimetry and ship depth soundings, *Science*, *277*, 1956–1962, doi:10.1126/science.277.5334.1956.
- Tanaka, K. (2010), Atmospheric pressure-wave bands around a cold front resulted in a meteotsunami in the East China Sea in February 2009, *Nat. Hazards Earth Syst. Sci.*, *10*, 2599–2610, doi:10.5194/nhess-10-2599-2010.
- Tintoré, J., D. Gomis, S. Alonso, and D. P. Wang (1988), A theoretical study of large sea-level oscillations in the western Mediterranean, *J. Geophys. Res.*, *93*, 10,797–10,803, doi:10.1029/JC093iC09p10797.
- Vidal, C., R. Medina, S. Monserrat, and F. L. Martín (2000), Harbor resonance induced by pressure-forced surface waves, in *Coastal Engineering 2000: Conference Proceedings*, pp. 3615–3628, Am. Soc. of Civ. Eng., Reston, Va., doi:10.1061/40549(276)282.
- Vilibić, I., S. Monserrat, A. B. Rabinovich, and H. Mihanović (2008), Numerical modelling of a destructive meteotsunami of 15 June, 2006 on the coast of the Balearic Islands, *Pure Appl. Geophys.*, *165*, 2169–2195, doi:10.1007/s00024-008-0426-5.

A. Jansá, AEMET, Moll de Ponent s/n, E-07014 Palma de Mallorca, Spain.

L. Renault, SOCIB, ICTS, Parc Bit, Naorte, Bloc A 2^op. pta. 3, Palma de Mallorca, Spain. (lrenault@imedea.uib-csic.es)

J. Tintoré and G. Vizoso, IMEDEA, UIB, CSIC, C/ Miquel Marquès, 21, E-07190 Esporles, Spain.

J. Wilkin, Institute of Marine and Coastal Sciences, Rutgers, State University of New Jersey, 71 Dudley Rd., New Brunswick, NJ 08901, USA.